Dianilides of Dipicolinic Acid Function as Synthetic Chloride Channels

Carl R. Yamnitz,[a] Saeedeh Negin,[b] I. Alexandru Carasel,[a]
Rudolph K. Winter[b] and George W. Gokel[a,b]*

Supplemental Information

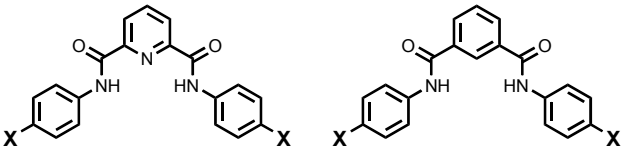

1: X = CH_3 **2**: X = H
3: X = CN **4**: X = NO_2

5: X = H
6: X = NO_2

Experimental

General. All NMR spectra were recorded on a Bruker Avance 300 spectrometer at 300 MHz and all chemical shifts are reported in ppm (δ), calibrated to literature values for internal non-deuterated solvent (CH_2Cl_2 or $CH_3S(O)CH_3$). All Mass Spectrometry experiments were performed on a JEOL MStation, JMS-700, double focusing high-resolution instrument. All fluorescence spectra and fluorescence quenching data were recorded on a Perkin Elmer LS50B Luminescence Spectrometer. Planar bilayer conductance measurements were performed with a Warner bilayer clamp instrument. All UV-Vis absorbance spectra were recorded on a Beckman Coulter DU 7400 Spectrophotometer. Calculations were run using the Spartan 2006 software package on a Dell Dimension DXP061 desktop with a 2.40GHz Intel® Core™2 Processor and 2.00GB of RAM.

Synthesis and of hosts 1-6, General Procedure. Unless otherwise stated, all chemicals were purchased from Sigma-Aldrich (St. Louis, MO). All solvents used were freshly distilled and all reactions were performed under an inert nitrogen atmosphere The commercially-available diacid chloride (2,6-pyridinedicarbonyldichloride for **1-4**, isophthaloyl chloride for **5** and **6**) was dissolved in acetonitrile (~2mmol in 7mL) and added drop-wise to a stirring solution containing an excess of the appropriate aniline in acetonitrile (~7mmol in 7mL) and triethylamine (5mL) held at 0°C in an ice bath. After addition, the mixture was returned to room temperature and then heated to reflux for 3h. After returning to room temperature, the solid was filtered and washed with acetonitrile and dried under high vacuum yielding the final product. All melting points, MS, ^1H and ^{13}C NMR values agree with the reported literature values.

Gas-phase binding calculations and molecular modeling. A lowest energy conformation search was performed using the Monte-Carlo simulated annealing method with the MMFFaq force field to yield the ten lowest energy conformers for each host and complex modeled. The geometry of each of these conformers were optimized by the density-functional B3LYP method using the 6-31G* basis set. Single-point energy calculations were performed using the same method and basis set to determine the overall lowest energy conformer (LEC). Binding energies were determined for each complex by adding the calculated energies of the host LEC and guest then subtracting the calculated energy of the complex LEC.

The channel model was created using two different DFT geometry optimized "subunits." The first, "A" is comprised of a molecule of **4** with a water molecule. The second, "BB" is made up of two molecules of **4** with four water molecules and a chloride anion. Altogether, the stack is composed of four units of "A" and three units of "BB" (equaling ten molecules of **4**, sixteen water molecules, and three chloride anions) aligned as A-BB-A-BB-A-BB-A.

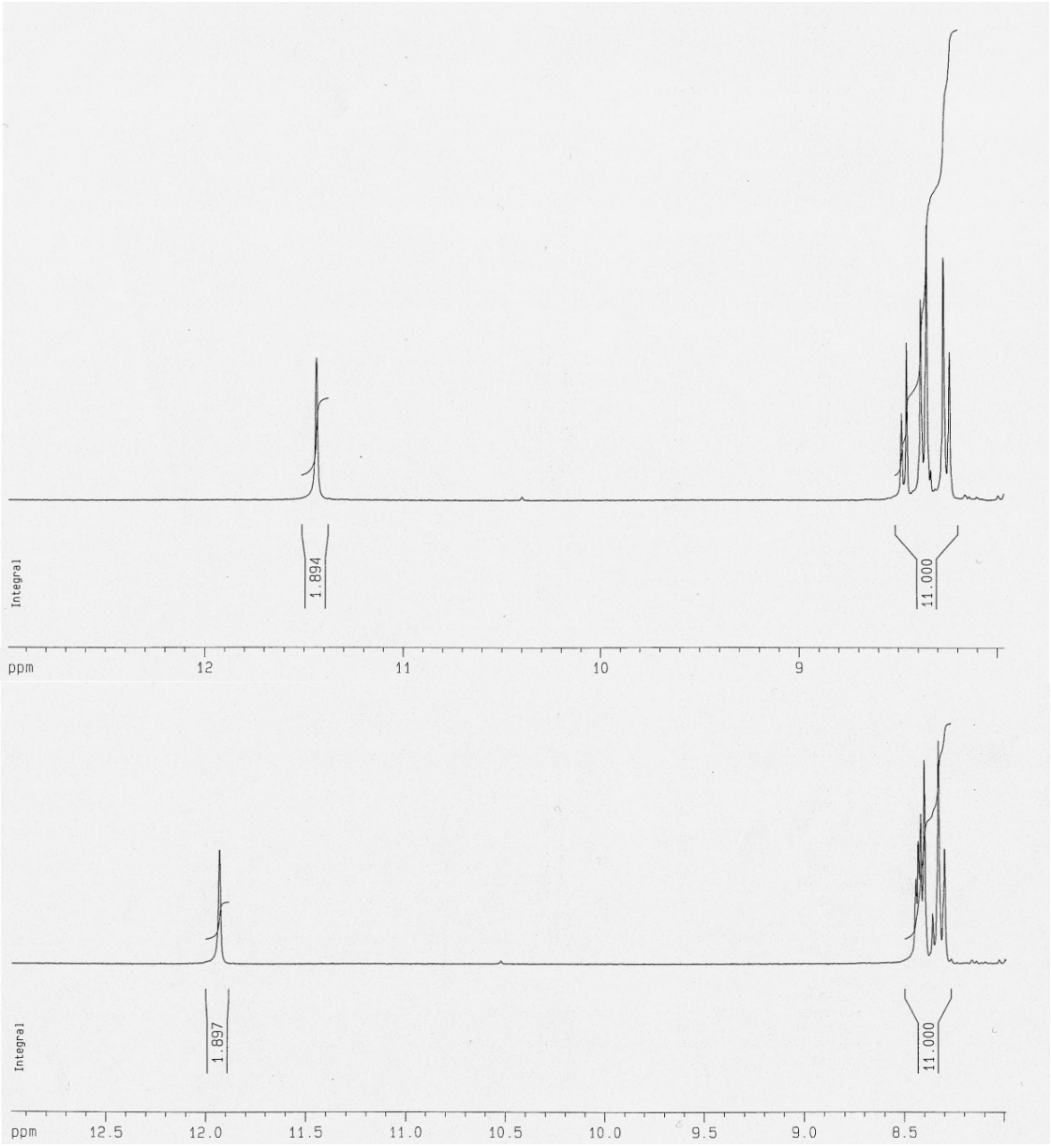

Chloride binding constants from ^{1}H-NMR titrations. Solutions of the receptor molecule in DMSO-d_6 were prepared at a concentration of 1.8 mM. A 1 mL solution thus prepared was transferred to a glass NMR tube and titrated with 18 mM solutions (10 equiv.) of $NBu_4^+Cl^-$, which contained host at the same concentration as the titrated solution. The chemical shifts of the NH protons were monitored as a function of the anion concentration until saturation was reached. Using data accrued from a minimum of three independent determinations, the association constants were calculated using a nonlinear regression analysis (GraphPad) with a curve fit for 1:1 binding originally used by Kavallieratos *et al*.[5b] Above are representative spectra showing the shift of the amide proton peak of **4** upon addition of Bu_4NCl guest. The uppermost panel is the spectrum with no guest present (δ NH = 11.438 ppm). The lower panel is the spectrum acquired with 2 equivalents of guest present (δ NH = 11.933 ppm).

Competitive chloride binding assayed by electrospray mass spectrometry. In each experiment, competing hosts were present in equimolar concentrations (50 μM) and chloride (as NBu_4Cl salt) was kept sub-stoichiometric (5 μM) so that competition for the guest would be obvious. The excess neutral host molecules are not observed unless complexed by Cl^-, so excess host could be ignored. The ratios shown in Table 1 were calculated from the total integration of relevant M/z peaks for host-Cl^- adducts. Five charged adducts were observed at significant abundances: $[host^A \bullet Cl]^-$, $[host^B \bullet Cl]^-$, $[(host^A)_2 \bullet Cl]^-$, $[(host^B)_2 \bullet Cl]^-$, and $[host^A \bullet host^B \bullet Cl]^-$, and total relative abundances were calculated for both hosts . In every case, the total relative abundance of the unsubstituted isophthalamide, **5**, was normalized to 1, with a value established for the competing compound. Errors are the calculated standard deviations of ratios from at least three independent experiments. Representative spectra for the competitions of 1:5, 4:5 and 6:5 follow with peaks of interest labeled.

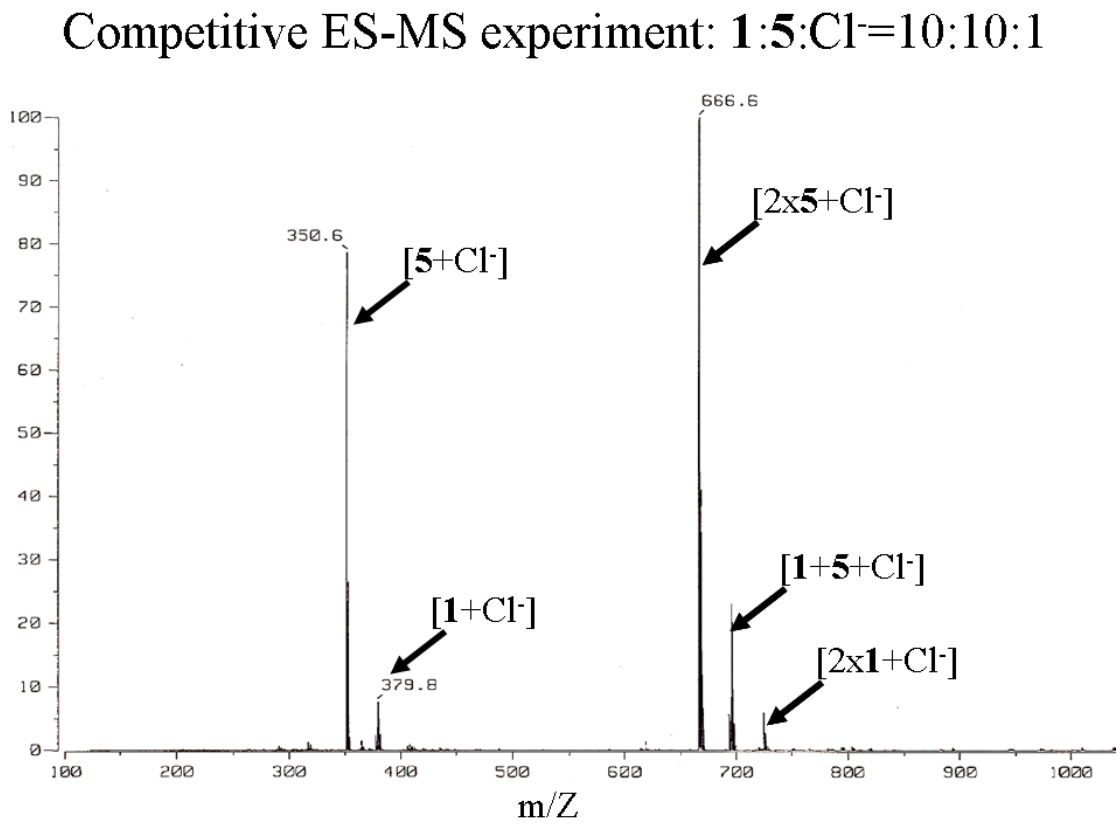

Competitive ES-MS experiment: **4**:**5**:Cl^-=10:10:1

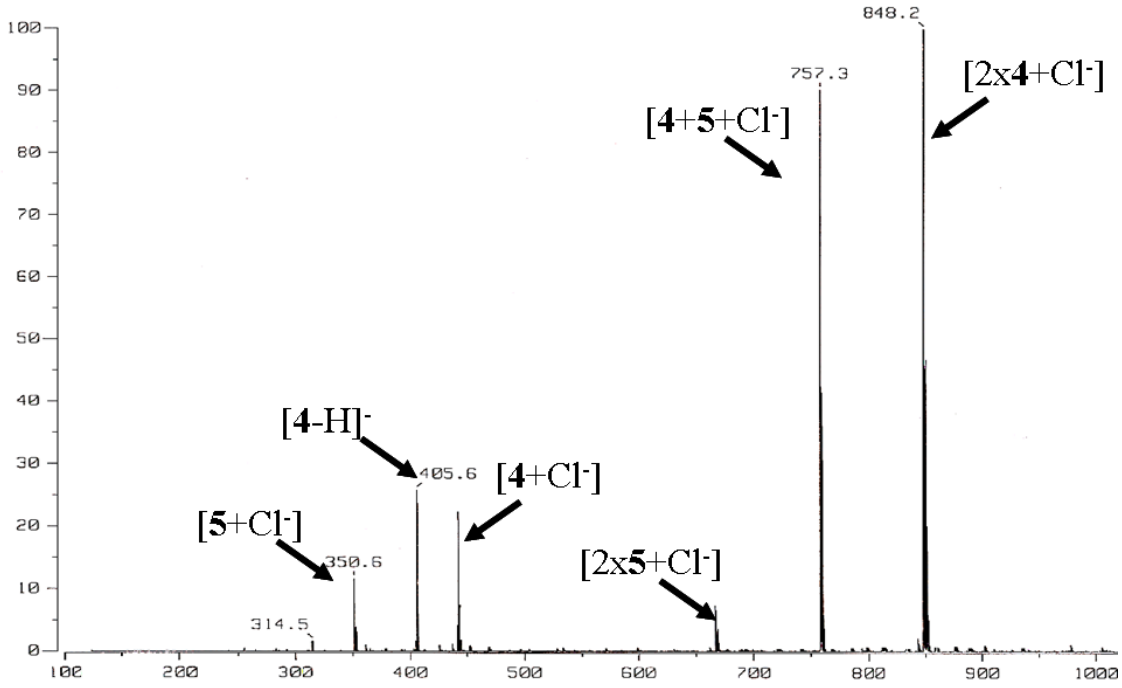

Competitive ES-MS experiment: **6**:**5**:Cl^-=10:10:1

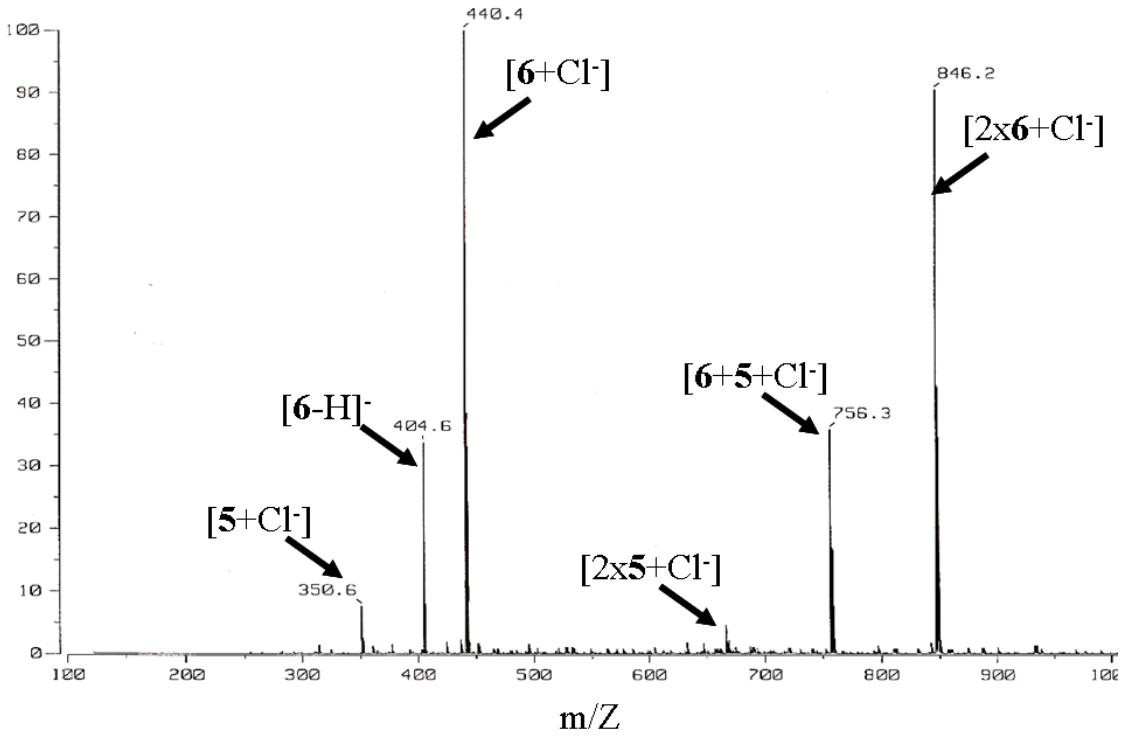

Preparation of phospholipid vesicles. 3.6mL of a 25 mg mL^{-1} chloroform solution of dioleoylphosphatidylcholine (DOPC, from Avanti Polar Lipids; Alabaster, AL), was distributed equally to 6 test tubes before evaporating the solvent *in vacuo* for 4 hours to yield dry films of 15mg each. For each vesicle preparation, a dry film sample was dissolved in a mixture of Et_2O (375 μL) and aqueous 1 mM lucigenin – 225mM $NaNO_3$ (375 μL). The combined mixture was sonicated for 30s yielding a yellow suspension. The diethyl ether was removed under low vacuum at 30°C for 2 to 2.5 hours. The resulting aqueous suspension was extruded through a 200 nm pore-size membrane filter 5 times. The filtered suspension was passed through a Sephadex G25 size exclusion column that was previously equilibrated with a 225mm $NaNO_3$ external buffer, collecting the first translucent fractions. This process effectively eliminated undesired extra-vesicular lucigenin as well as micelles and vesicles of a smaller-than-desired size. The size of the resulting purified vesicles was confirmed by light-scattering analysis, and the sample was diluted to the appropriate concentration using 225mm $NaNO_3$ external buffer.

Lucigenin quenching assay. A 2 mL aliquot of 0.31 mM vesicles in external buffer was placed in a quartz cuvette to be used for the lucigenin quenching experiment. The excitation wavelength was set to 368 nm and the emission wavelength to 506 nm, with both slits set to 5 nm. After a brief initial equilibration phase, 100 μL of a 4 M NaCl solution were added in order to create a chloride gradient between the outside (190 μM) and the inside (0 μM) of the vesicles. When the fluorescence intensity stabilized, 2 μL of the desired compound at the appropriate concentration (10 mM stock solution for studies with 10 μM concentrations) in DMSO were added. At the end of each experiment the vesicles were lysed with 100 μL of a 2% Triton X-100 solution to establish the level of baseline fluorescence. The data displayed is the average of a minimum of three independent trials, are baseline –corrected and normalized to the initial fluorescence intensity, $F_0 = 1$.

Planar bilayer conductance. Membranes were formed by painting lipid solutions (asolectin from soybean dissolved in *n*-decane, 25mg mL^{-1}) over a 200 μm aperture separating two chambers containing 3.000 mL buffer solutions (450 mM KCl, 10 mM HEPES, pH = 7.00). 21μL of a DMSO solution of the appropriate transporter was then added into the *cis* chamber (the side of the membrane that hosts the input electrode) to yield a final concentration of 7 μM. Working in a Faraday cage (Warner Instruments) at room temperature, specific potentials were applied between two electrodes immersed in the two buffer solutions. The resulting currents were amplified (amplifier BC-525 D, from Warner Instruments), filtered with a 4-pole Bessel filter at 1 kHz, digitized by Digitizer (Digidata 1322A from Axon Instruments), sampled at 100 Hz amplifier filter frequency and collected using Clampex 9.2 (Axon Instruments). The data were analyzed later using Clampfit 9.2 (Axon Instruments).

Fluorescence of compound 4. Fluorescence emission intensity was found to be maximal for all wavelengths with λ_{ex} = 280 nm when both slits were set to 5 nm. The fluorescence emission spectrum was recorded while titrating a solution of host in 1% DMSO/Water into a solution of either 1% DMSO/Water or 1% DMSO/Water with 0.17mM DOPC vesicles. In all cases, the recorded spectra are the average of 10 scans per concentration per trial with a minimum of three independent trials totaling a minimum of 30 scans.

Supplementary Figures and Discussion

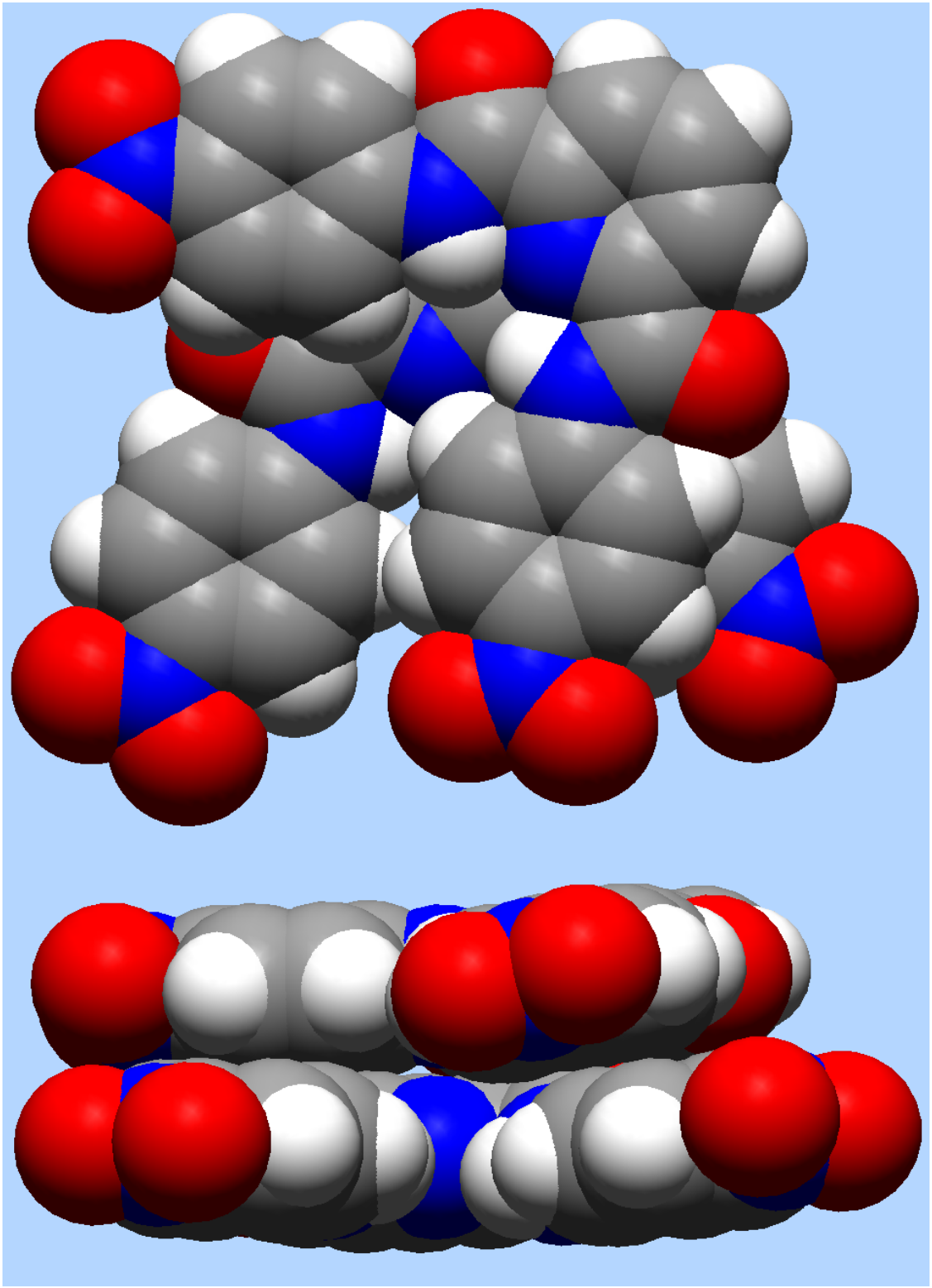

Fig.S1 *Orthogonal depictions of the solid-state structure of the DMSO pseudo-polymorph of* ***4****, derived from the work of Yin et al. (CSD:NEDSAR).*

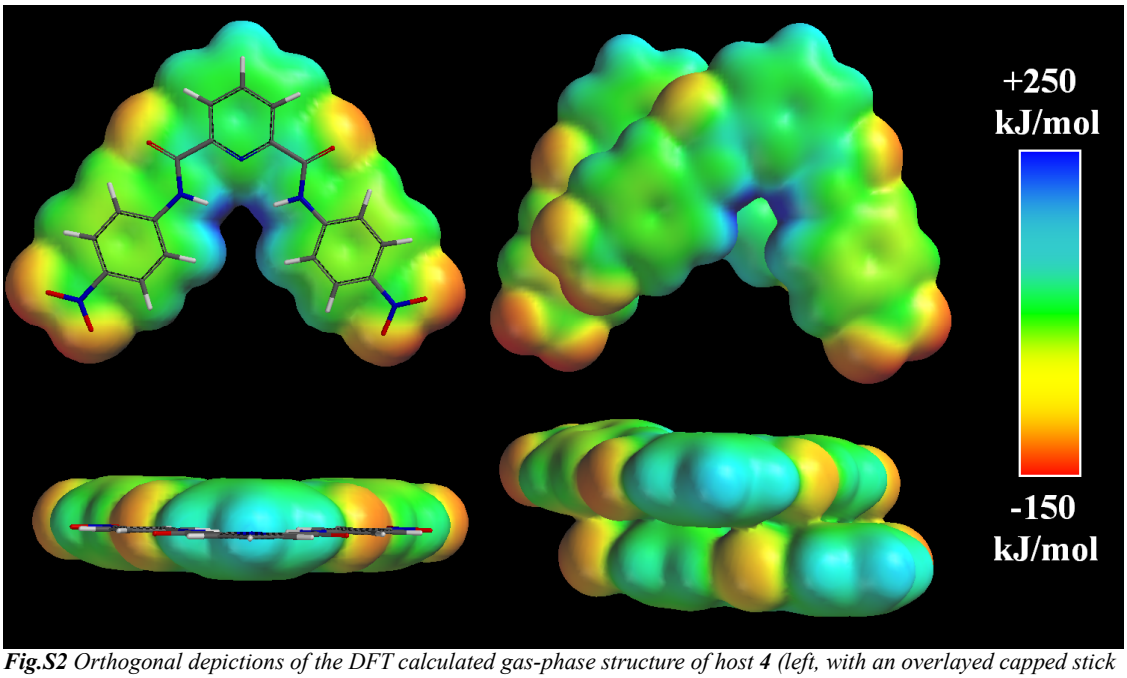

Fig.S2 *Orthogonal depictions of the DFT calculated gas-phase structure of host* ***4*** *(left, with an overlayed capped stick structure), and its homodimer (right).*

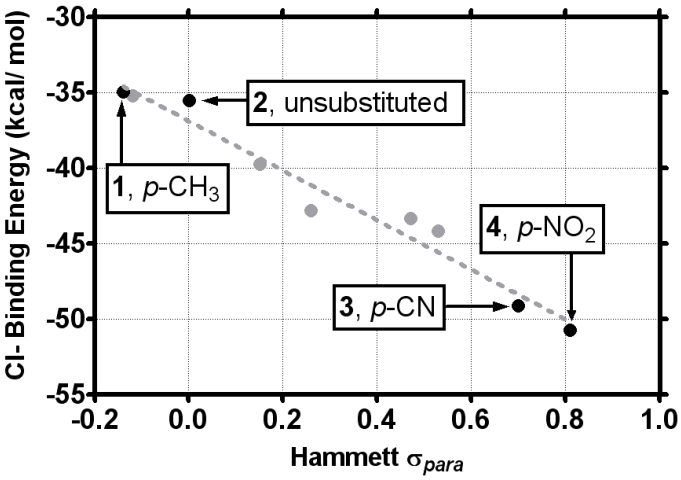

Fig.S3 *DFT-Calculated chloride binding energies of nine different para-substituted dipicolinamides (including hosts* ***1-4****) plotted against their Hammett constants. The data points fit a line (R^2 = 0.96) and show indicate that the dipicolinamides with more electron-withdrawing substituents would serve as better chloride binders.*

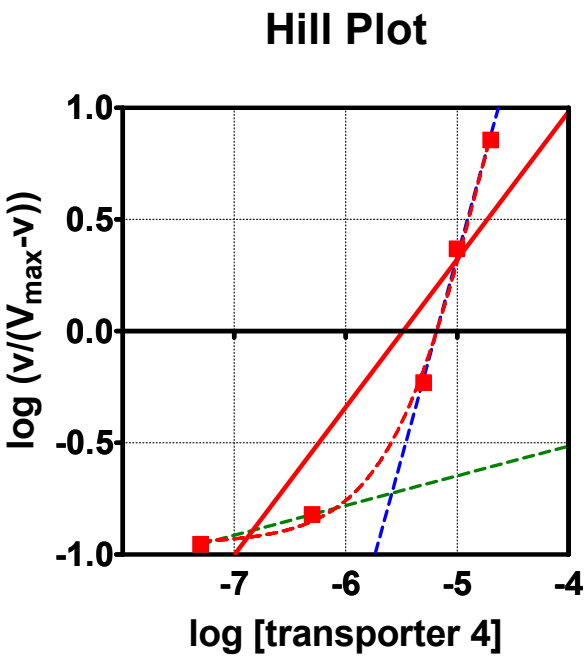

Fig.S4 *A Hill plot derived from the data presented in Fig. 1b (variation of* ***[4]****) via application of the Stern-Volmer equation.*

Hill Plot: Concentration Dependence of Carrier and Channel Mechanism of Transport. Examination of the Hill plot derived from the quenching data seen in Figure 1b (variation of **[4]**), shows that both carrier and channel mechanisms may be at work. If all 5 points were fit to a single straight line (red full line), as normally done with a Hill plot, a slope of 0.66 is the result, indicating a competitive concentration dependence that is characteristic of carriers. However, if the plot were divided into two parts, the first with the two lowest concentrations and the second with the three remaining, two straight lines result: the first half yielding a slope of 0.13 (green dashed line) and the second a slope of 1.98 (blue dashed line), indicating a competitive and synergistic concentration dependence, respectively. Presumably, these two straight lines are a simplification, and a non-linear relationship is truly at work (red dashed line) with both carrier activity and channel activity present at once, but with only 5 data points, this is merely an assumption. Further study of this phenomenon, using far more than 5 concentrations is under current investigation.

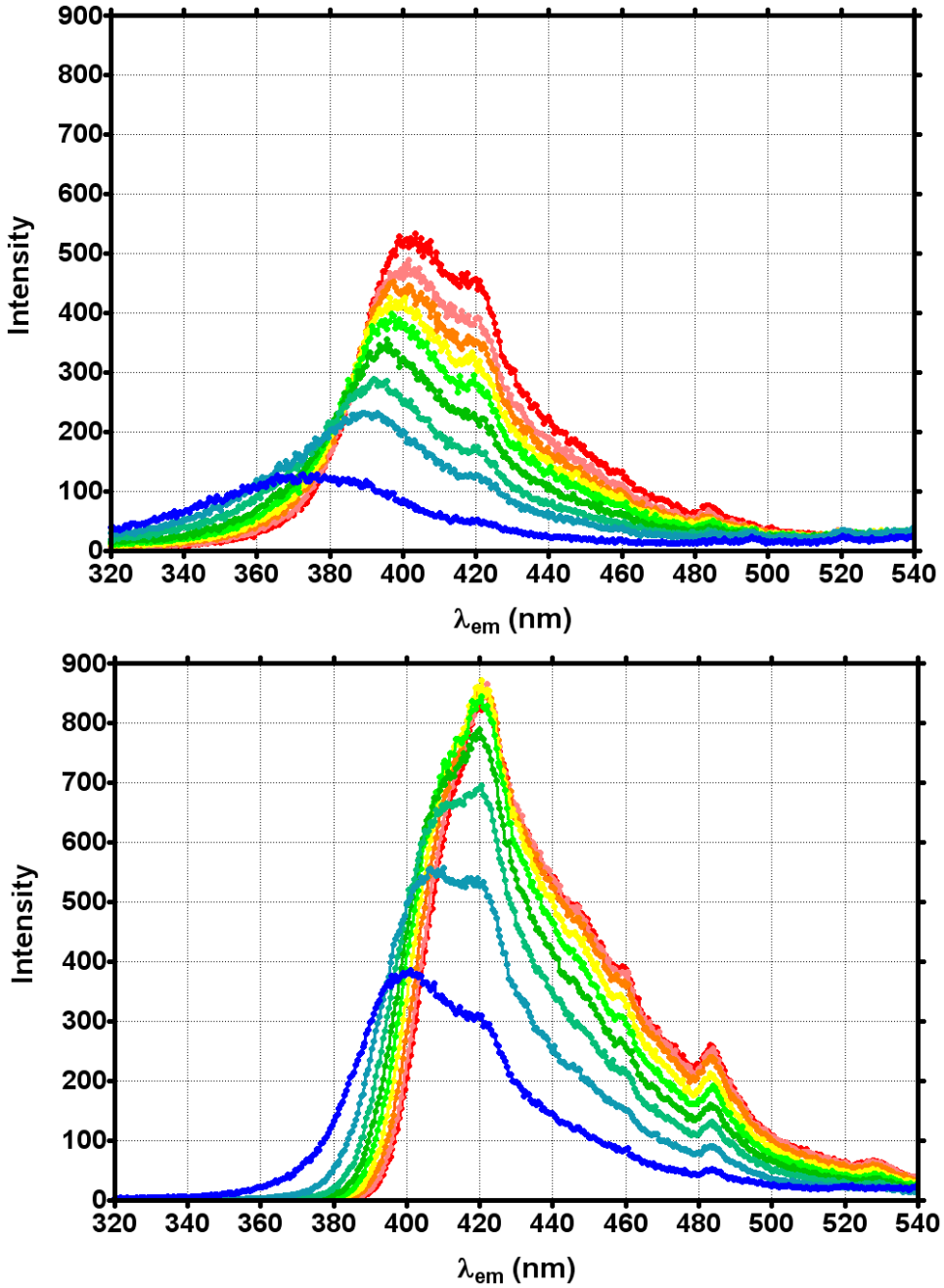

Fig.S5 *Full expansions of Fig. 1f,g showing the fluorescence spectra of* ***4*** *at concentrations ranging from 10 μM (dark blue trace) to 90 μM (red trace) both in 1% DMSO/H_2O solution only (top) and in 1% DMSO/H_2O solution with 0.17mM DOPC vesicles (bottom). The spectrum for 10 μM with vesicles nearly overlaps the spectrum for 40 μM without vesicles. 4 different species can be elucidated: the first fluorescing at ~400nm, the second at ~420nm, a third at ~485 nm and a fourth at ~ 530nm. These species could correspond to different oligomerization states.*

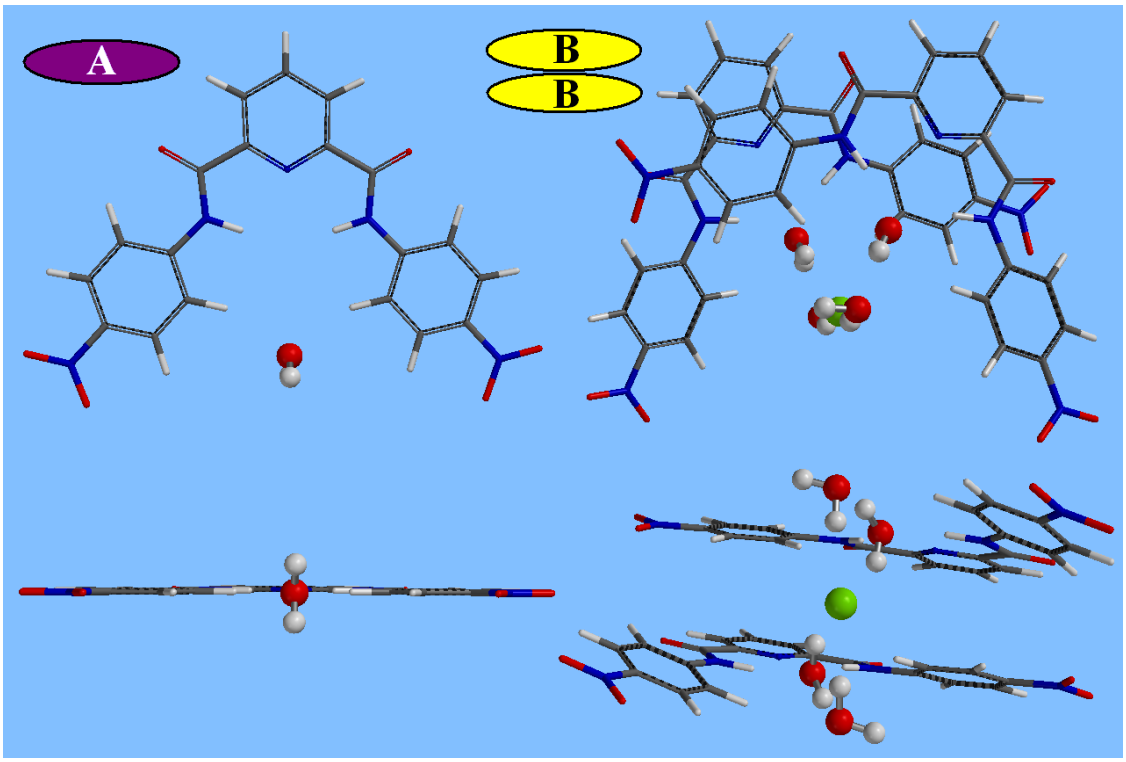

Fig.S6 *Geometry optimized (DFT, B3LYP/6-31G*) structures of (left)* ***4*** *• H_2O and (right) (2x)* ***4*** *• (4x) H_2O • Cl^-. These structures were used as subunits "A" and "BB," respectively, in building the channel model.*

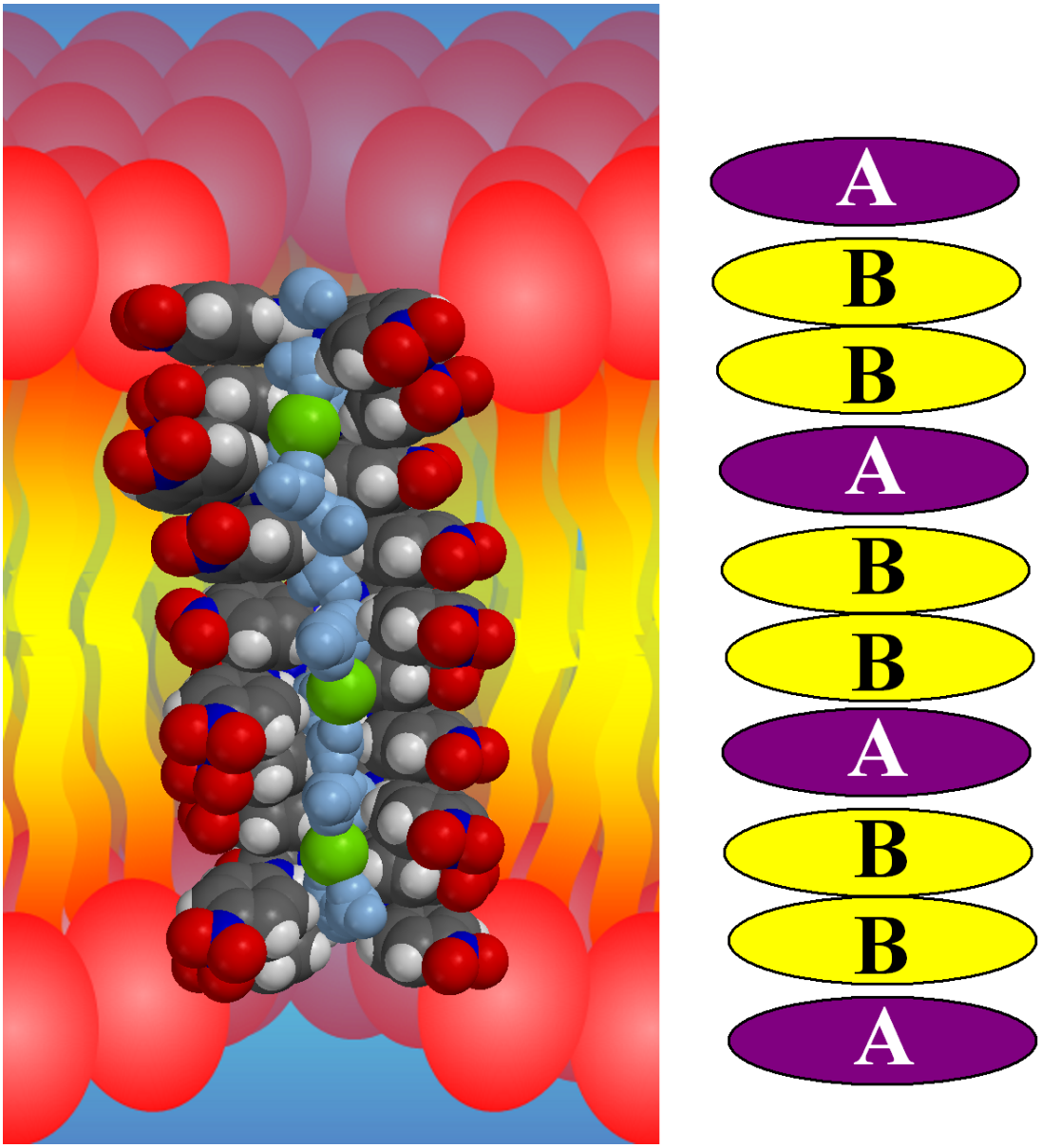

Fig.S7 *(Left) Expansion of Fig. 1h showing a stack of 10 molecules of* ***4****, 3 chloride anions, and 16 water molecules. The distance between the most distal monomers in the stack is approximately 34Å. The channel was modeled using the DFT-calculated geometries of 4x "A" and 3x "BB" subunits shown in Fig. S6 arranged as shown (right) before applying an MMFFaq energy minimization method for geometry optimization.*